PRAMANA — journal of physics

Vol. 79, No. 4
October 2012
pp. 737–752

Heavy ions: Report from Relativistic Heavy Ion Collider

SONIA KABANA

SUBATECH, Laboratoire de Physique Subatomique et des Technologies Associees,
4 rue Alfred Kastler, BP 20722, 44307 Nantes Cedex 3, France
E-mail: kabana@mail.cern.ch

Abstract. We review selected highlights from the experiments at the Relativistic Heavy Ion Collider (RHIC) exploring the QCD phase diagram. A wealth of new results appeared recently from RHIC due to major recent upgrades, like for example the Υ suppression in central nucleus–nucleus collisions which has been discovered recently in both RHIC and LHC. Furthermore, we discuss RHIC results from the beam energy scan (BES) program aiming to search for a possible critical point and to map out the QCD phase diagram.

Keywords. Heavy-ion collisions; quark gluon plasma; QCD phase diagram.

PACS Nos 25.75.−q; 25.75.Ag; 25.75.Cj; 25.75.Dw; 25.75.Gz; 25.75.Ld; 25.75.Nq

1. Introduction

Experiments using ultrarelativistic heavy-ion collisions study nuclear matter under extreme conditions of density and temperature. They aim to reproduce a phase transition between states with hadronic and partonic degrees of freedom, the latter corresponding to the so-called quark gluon plasma. This phase transition is believed to have taken place 10^{-6} s after the Big Bang. QCD on the lattice predicts a cross-over at baryochemical potential $\mu_{\mathrm{B}} = 0$ at temperature of 150–190 MeV, while at higher μ_{B} a possible first-order phase transition line ending in a critical point is envisaged [1]. Figure 1a shows the temperature as a function of the chemical potential μ_{B}, and summarizes present ideas of the QCD phase diagram, several aspects of which wait to be verified by experiments.

Selected historical milestones of the search for the QCD phase transition are firstly, the 'discovery of a new state of matter', announced by CERN in 2000 [2] based on results from CERN SPS experiments exhibiting a suppression of Ψ' and J/ψ, the measurement of enhanced strange meson and baryon production, the estimate of the temperature (T) of direct photons from the plasma as 335 MeV, the estimate of the temperature at chemical freeze-out being T(chem.fr.out) = 170 MeV [3,4] being near to the predicted T_{c} and to the Hagedorn limiting temperature [5] and other observations made in central $A + A$ collisions at $\sqrt{s_{NN}} = 17{,}19$ GeV. The average initial Bjorken energy density ε reached at SPS is about 3.5 GeV/fm^3, and is larger than the predicted critical energy density for the QCD phase transition.

DOI: 10.1007/s12043-012-0384-4; ***e*Publication: 12 October 2012**

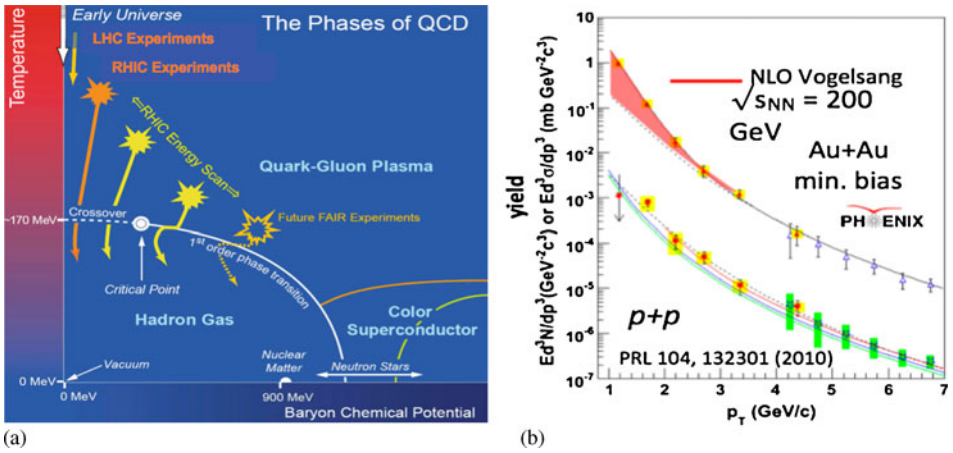

Figure 1. **(a)** QCD phase diagram of temperature as a function of the baryochemical potential. **(b)** Invariant cross-section ($p + p$) and invariant yield (Au + Au) of direct photons as a function of p_{T} at $\sqrt{s_{NN}} = 200$ GeV (see [6,7] for more details).

The second milestone was the 2005 BNL announcement of results from the four RHIC experiments, featuring the discovery of the 'strongly interacting quark gluon plasma' (sQGP) state built in central Au+Au collisions at $\sqrt{s_{NN}}$ up to 200 GeV reaching an average initial Bjorken energy density of about $\varepsilon = 5$ GeV/fm^3 [8]. The 'jet quenching' phenomenon was discovered at RHIC and measurements have shown that the matter built in central Au+Au collisions is consistent with a 'perfect liquid', a non-anticipated result. The results from RHIC marked a new era in QCD studies, and allowed new frontiers of QCD to be explored, for example comparisons of data to model prediction using the AdS/CFT correspondance.

The third milestone is marked by results coming out in the last 1–2 years, with the start of the LHC experiments studying Pb+Pb collisions at $\sqrt{s_{NN}} = 2.76$ TeV [9] as well as a wealth of new results coming from RHIC due to recent important upgrades of the accelerator and the experiments. The average initial Bjorken energy density ε reached in Pb+Pb collisions at LHC is about 16 GeV/fm^3, and is well above the predicted critical energy density for the QCD phase transition.

Concerning the critical parameters of the QCD phase transition, several observables [10–13] suggest that the onset of phase transition in $A + A$ collisions may be well below $\sqrt{s_{NN}} = 17$ GeV which is the top SPS energy for Pb+Pb collisions, and in the region of an energy around $\sqrt{s_{NN}} = 10$ GeV for Pb+Pb collisions, corresponding to an initial energy density of ε(init, Bjorken) = 0.5–1 GeV/fm^3, in the vicinity of predictions from lattice QCD.

This motivated a beam energy scan at CERN as well as at RHIC, to scan collision energies from below T_{c} until the highest available energies. The beam energy scan at RHIC aims to study the onset of the phase transition, to search for a possible critical point and map out the QCD phase diagram. The collision systems taken up to now are Au+Au collisions at 7.7, 11.5, 19.6, 27, 39, 62, 130, 200 GeV and Cu+Cu collisions at 22.4 GeV.

There are two experiments at RHIC taking data at present, PHENIX and STAR. In the following we present selected highlights of recent PHENIX and STAR experimental results on direct thermal photons, flow, jet quenching, open and hidden charm and beauty, antimatter, and results from the RHIC beam energy scan.

2. Direct thermal photons

Thermal photons emitted from a plasma of partons allow for a measurement of its temperature. The PHENIX experiment has measured an excess of direct photons produced in minimum bias and central Au+Au collisions at 200 GeV at transverse momenta $p_T < 2.5$ GeV/c, as compared to those measured in $p + p$ collisions at 200 GeV scaled by the number of binary collisions (figure 1b) [7].

Direct photon production in $p + p$ collisions is well described by NLO calculations. The excess direct photons at low p_T in Au+Au collisions exhibit an exponential spectrum consistent with radiation from a thermal source. The measured inverse slope is 220 ± 20 MeV, while the temperature of the thermal source of those photons is estimated to be $T = 300$–600 MeV, depending on the thermalization time assumed [7]. The possibility that the excess seen is related to cold nuclear matter effects has been excluded by recent PHENIX data on direct photons in d+Au collisions which do not show an excess over $p + p$ data scaled with the number of binary collisions [14].

The RHIC measurement is the first firmly established measurement of the temperature of direct thermal photons from the quark gluon plasma. This temperature of about 4 trillion degrees Celsius is about 250,000 times hotter than the centre of the Sun and is higher than the predicted critical temperature for the QCD phase transition.

3. Flow

An important information constraining hydrodynamic models is the amount of elliptic flow exhibited by direct photons. The flow strength indicates whether the photons are emitted earlier or later. In particular the flow is expected to be smaller at earlier times and larger at later times. Figure 2a shows the measured direct photon elliptic flow, v_2, as a function of p_T for the 20% most central Au+Au collisions at $\sqrt{s_{NN}} = 200$ GeV [15]. For a discussion on flow, see [16]. In the low p_T region, where thermal photons dominate (figure 1) the flow is large, and it is comparable to the flow of hadrons [17] at $p_T = 2$ GeV, even though systematic errors are very large. The flow approaches zero with increasing p_T particularly in the region where prompt photons are expected to dominate. The measured elliptic flow is larger than the hydrodynamic calculations shown in figure 2a, presenting a challenge to theoretical calculations, aiming to describe at the same time the p_T dependence as well as the elliptic flow of the direct photons in Au+Au collisions.

Other important information that can be used to extract properties of the sQGP such as the viscosity-to-entropy ratio, are the higher order moments of flow. Collision geometry fluctuations excite higher order moments of the flow, which can be compared to models in order to learn about the properties and the initial state of the medium [6,23,24].

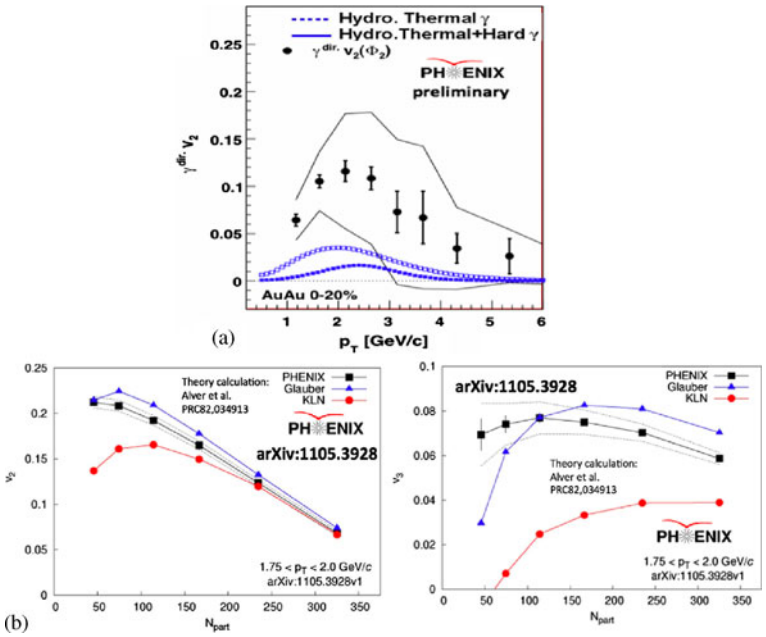

Figure 2. **(a)** PHENIX measurement of direct photon elliptic flow v_2 as a function of p_T in the 20% most central Au+Au collisions at $\sqrt{s_{NN}} = 200$ GeV [15]. The error bars indicate the statistical and the lines the systematic uncertainty. The data are compared to a hydrodynamical calculation. The open symbols (upper line) only include thermal photons. The closed symbols (lower line) also take prompt photons into account [6]. **(b)** *Left plot*: v_2 as a function of N_{part} [18]. *Right plot*: v_3 as a function of N_{part} [18]. The data are compared to two hydrodynamical calculations [19], one with a Glauber initial state (MC-Glauber) [20] and the other with a saturation or colour glass condensate (CGC) initial state (MC-KLN) [21,22].

Figure 2b shows the v_2 (left plot) and v_3 (right plot) flow coefficients in Au+Au collisions at $\sqrt{s_{NN}} = 200$ GeV as a function of centrality and p_T measured by PHENIX [18]. The data are compared to two hydrodynamical calculations [19]. One has a Glauber initial state (MC-Glauber) [20] and a value of $\eta/s = 1/4\pi$, which is the AdS/CFT conjectured quantum lower bound [25,26]. The other has a saturation initial state (MCKLN) [21,22] and a value for the viscosity-to-entropy ratio of $\eta/s = 2/4\pi$. Both models describe the v_2 data reasonably well, in particular for the points with more central collisions where hydrodynamics is expected to work.

Figure 2b (right plot) compares the v_3 coefficient as a function of N_{part} [18] and the v_3 obtained from the same two hydrodynamical calculations described above. It is observed that the v_3 coefficient allows to disentangle between the two models, in particular the MC-Glauber assumption and $\eta/s = 1/4\pi$ falls nearer to the data than the MC-KLN model which underestimates the data. This illustrates that simultaneous measurement of different flow harmonics helps to better constrain the initial state and η/s estimates.

4. Jet quenching

Partons going through a dense and hot sQGP medium interact with the medium and loose energy through e.g. gluon radiation. This phenomenon known as jet quenching, allows for an estimate of the gluon density of the medium. To extract this information using models, it is important to understand the mass, path length and collision energy dependence of jet quenching through systematic comparisons of data to models, and understand the origin of the energy loss mechanism involved. For example, it is expected that radiative energy loss is smaller for larger quark masses [27,28]. The collision energy dependence and the medium path length dependence are constraining the models further.

One way to quantify jet quenching is via the nuclear modification factor $R_{\rm AA}$, defined as the particle yield in $A + A$ collisions divided by the particle yield in $p + p$ collisions at same energy scaled up to the number of binary collisions. When no jet quenching is observed, $R_{\rm AA} = 1$. Figure 3a shows that the $R_{\rm AA}$ of several mesons at high $p_{\rm T}$ in Au+Au collisions at 200 GeV exhibits a suppression by a factor of about 5, namely down to $R_{\rm AA} = 0.2$, while direct photons in the region of $p_{\rm T}$ up to 13 GeV are consistent with no quenching ($R_{\rm AA} = 1$).

We shall discuss in the following sections the collision energy dependence, the medium length dependence and the mass dependence of the jet quenching.

Figure 3b shows that $R_{\rm AA}$ at high $p_{\rm T}$ is similar for π^0 measured by PHENIX in Au+Au collisions at $\sqrt{s_{NN}} = 200$ GeV, and for charged hadrons measured by ALICE in Pb+Pb collisions at $\sqrt{s_{NN}} = 2.76$ TeV, even though the Bjorken initial energy density of the medium at LHC is estimated to be larger than at RHIC. All measurements shown in this figure correspond to the most central collisions. We discuss further the energy dependence towards lower collision energies in §7.

To study the path length dependence of parton energy loss in the medium, one can for example select collisions of different centrality. Figure 4a shows the flow coefficient v_2 and the $R_{\rm AA}$ factor for high $p_{\rm T}$ π^0 produced in Au+Au collisions at 200 GeV as a function of the number of participants [6].

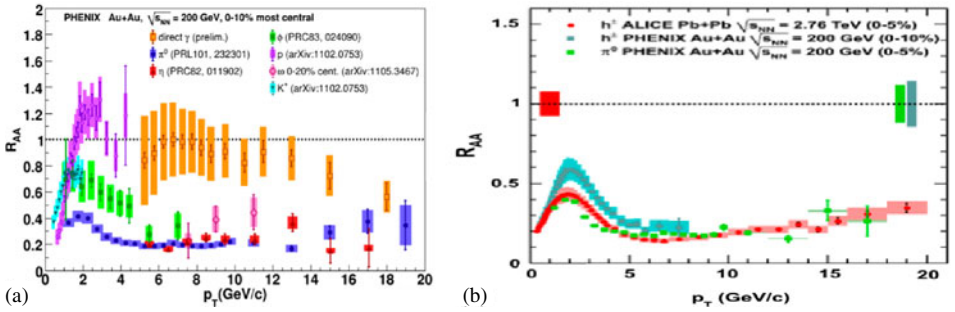

Figure 3. **(a)** Nuclear modification factor $R_{\rm AA}$ for several hadrons and direct photons as a function of $p_{\rm T}$ in Au+Au collisions at $\sqrt{s_{NN}} = 200$ GeV from PHENIX [29]. **(b)** Nuclear modification factor $R_{\rm AA}$ for charged hadrons and neutral pions as a function of $p_{\rm T}$ in Au+Au collisions at $\sqrt{s_{NN}} = 200$ GeV from PHENIX, and charged hadrons in Pb+Pb collisions at $\sqrt{s_{NN}} = 2.76$ TeV from ALICE [29].

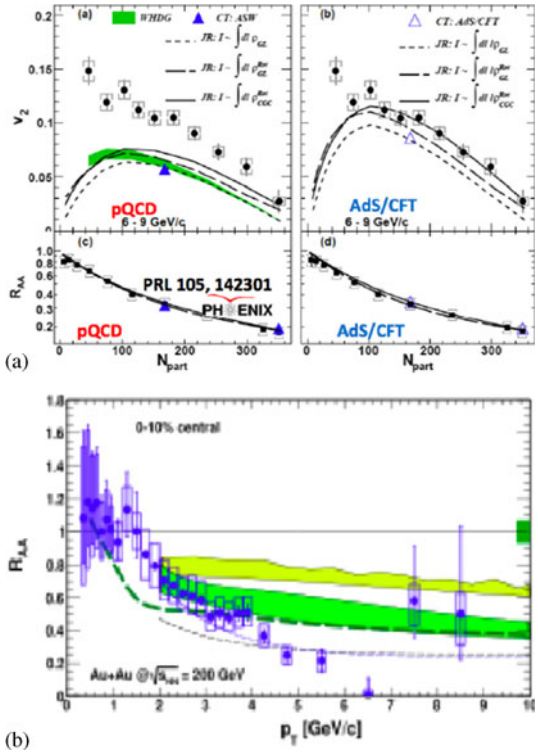

Figure 4. **(a)** *Lower two panels*: $R_{\rm AA}$ as a function of $N_{\rm part}$ [30]. The data are compared to two different model calculations [31,32] (see text for more details). *Upper two panels*: elliptic flow coefficient v_2, of high $p_{\rm T}$ π^0 production [30] compared to the same models. **(b)** $R_{\rm AA}$ of non-photonic electrons in central Au+Au collisions at $\sqrt{s_{NN}} = 200$ GeV as a function of $p_{\rm T}$ (see [33] for more details).

The data are compared to two model calculations shown separately in right and left plots of figure 4a [31,32]. The model on the left plot takes a linear or quadratic path length dependence of energy loss into account as would be expected from pQCD [34,35]. The model on the right plot assumes a cubic path length dependence as in AdS/CFT [36–38]. It is observed that the data on $R_{\rm AA}$ agree with both models, while the data on the v_2 coefficient underestimate the pQCD inspired model and agree well with the model assuming cubic path length dependence in the right plot for semiperipheral and central Au+Au collisions. It is therefore possible to discriminate between the different models on the path length dependence exploring the flow coefficients showing that the data favour the cubic path length dependence as expected within AdS/CFT models.

Concerning the parton mass dependence of jet quenching as mentioned earlier, one expects a hierarchy in the amount of energy loss observed while measuring the jet quenching of hadrons with beauty, charm and light and strange quarks. One of the most interesting results of RHIC has been the finding that this hierarchy is not observed in the data [33,39,40]. We shall discuss this in the next paragraph.

5. Open and hidden charm and beauty

5.1 *Open charm and beauty*

Open beauty (B) and charm (C) are prominent probes of the sQGP medium produced in central ultrarelativistic heavy-ion collisions. One of the most important results of RHIC is the suppression observed in the nuclear modification factor of non-photonic electrons from charm and beauty decays in central Au+Au collisions at 200 GeV [33,39,40]. Figure 4b shows R_{AA} for non-photonic electrons originating from charm and beauty decays measured by PHENIX in the most central Au+Au collisions at 200 GeV [33]. Similar results were obtained by STAR [40]. The R_{AA} for non-photonic electrons from heavy flavour decays is compatible with R_{AA} of charged mesons at high p_T. Therefore, no significant mass dependence is exhibited in the data. These data challenge the theoretical models and show the importance of a separate measurement of charm and beauty yields in Au+Au collisions at RHIC, which has motivated a program of silicon detector upgrades in both PHENIX and STAR.

The data on non-photonic electron from charm and beauty can be described better by models introducing, for example, collisional energy loss, running coupling constant and other modifications (for a discussion, see [33]). In addition to R_{AA}, the measurement of a non-zero v_2 coefficient of non-photonic electrons originating from charm and beauty decays offers an additional important constraint to models towards a better understanding of heavy flavour in Au+Au reactions at RHIC [33].

A relevant question to ask is if the observed suppression can be due partially or entirely to cold nuclear matter effects in Au+Au collisions. New preliminary data on non-photonic electrons from d+Au collisions at 200 GeV measured by PHENIX show that the modification factor R_{dAu}, defined as the yield in d+Au with respect to the yield in $p+p$ collisions scaled up to the number of binary collisions, does not show a suppression that can explain the suppression of non-photonic electrons in central Au+Au collisions as been due to cold nuclear matter effects [41].

Another important step has been achieved by separating the charm and beauty contributions in the non-photonic electron yield and the measurement of its p_T dependence in $p+p$ collisions at 200 GeV which has been measured by STAR and PHENIX. The beauty contribution in the non-photonic electrons is found to increase with p_T and becomes comparable to the charm contribution to non-photonic electrons at $p_T = 5$ GeV/c [42,43].

A combined analysis of R_{AA} of non-photonic electrons in high $p_T > 5$GeV/c in central Au+Au collisions at 200 GeV and of the beauty contribution to non-photonic electrons in $p + p$ collisions at 200 GeV also at high $p_T > 5$GeV/c, allowed to set limits separately on the nuclear modification factors of non-photonic electrons from open charm and beauty in Au+Au collisions. This is demonstrated in figure 5a which shows the nuclear modification factor of non-photonic electrons from beauty as a function of the nuclear modification factors of non-photonic electrons from charm, in high $p_T > 5$GeV/c and in central Au+Au collisions at 200 GeV [43]. This analysis has been performed using STAR and PHENIX data [43]. The R_{AA} for non-photonic electrons from beauty is less than 0.6 at the 90% confidence level even if non-photonic electrons from charm are completely suppressed. In this figure it is also demonstrated that models with only radiative energy loss are excluded by the data (model I).

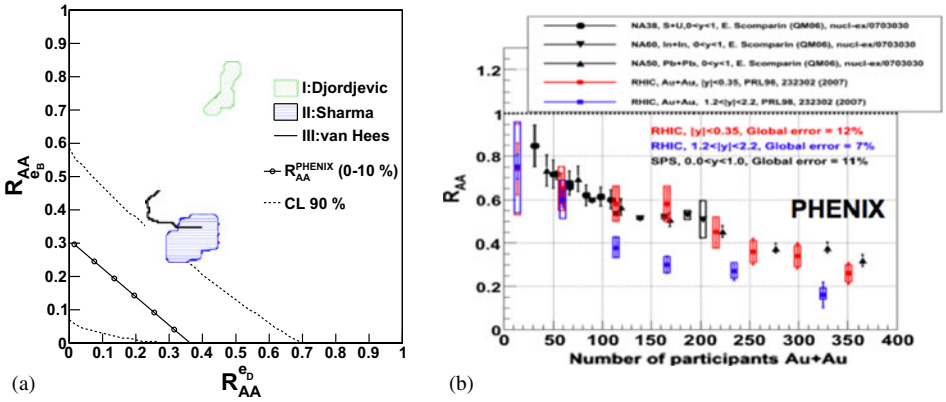

Figure 5. **(a)** 90% Confidence level (CL) contours for the nuclear modification factor R_{AA} for electrons from charm and beauty meson decays in central Au+Au collisions at $\sqrt{s_{NN}} = 200$ GeV and $p_{\mathrm{T}} > 5$ GeV compared to models [43]. **(b)** Nuclear modification factor R_{AA} for J/ψ as a function of N_{part} in Au+Au collisions at $\sqrt{s_{NN}} = 200$ GeV from PHENIX [46].

5.2 *Hidden charm and beauty*

Quarkonia can be suppressed by colour screening in the plasma, and different states have different dissociation temperatures [44,45]. The hierarchy of the suppression pattern of quarkonia can therefore serve as a QGP signature and as a thermometer of the quark gluon plasma formed in these collisions. Also, effects other than colour screening can contribute to the suppression of quarkonia, like e.g. suppression by hadronic comovers. In addition, quarkonia can be regenerated from $q\bar{q}$ pairs counteracting a possible suppression.

Figure 5b shows the R_{AA} for J/ψ in Au+Au collisions at 200 GeV as a function of the number of participants measured by PHENIX. It is shown that J/ψ at forward rapidity $1.2 < |y| < 2.2$ is more suppressed than J/ψ in midrapidity $|y| < 0.35$ [46]. This observation is contrary to that expected for supression due to colour screening since the suppression does not increase with the local density of the medium. The R_{AA} factor observed for J/ψ in Au+Au collisions at the most central events is smaller than 0.6 expected if J/ψ from ψ' and χ_{c} decays would be fully suppressed due to the dissociation of those states.

A very important measurement needed to understand J/ψ production in Au+Au collisions is the measurement of J/ψ R_{dA} factor in d+Au collisions at 200 GeV in order to estimate cold nuclear matter effects. The PHENIX Collaboration has measured recently the R_{dAu} and $R_{\mathrm{CP}} = (0-20\%)/(60-80\%)$ factors for the J/ψ production in d+Au collisions at 200 GeV as a function of rapidity. The R_{dAu} factor in central d+Au collisions and the R_{CP} factor exhibit a significant suppression in forward rapidity [47]. However, the rapidity and centrality dependence of these nuclear modification factors cannot be reconciled with a picture of cold nuclear matter effects, when an exponential or linear dependence on the nuclear thickness is employed and other effects like gluon saturation or initial-state parton energy loss may play an important role [47]. To establish possible

colour screening effects of J/ψ in Au+Au collisions, it would be important to correct for J/ψ suppression due to other sources than colour screening as a function of rapidity and p_{T} using d+Au data.

A possible interpretation of the J/ψ suppression pattern at RHIC assumes that J/ψ is not suppressed through colour screening at RHIC since its dissociation temperature is expected to be $2T_{\mathrm{c}}$. The suppression observed is then entirely due to the dissociation of the states χ_{c} and ψ' which have a dissociation temperature near T_{c}, as well as possible cold nuclear matter effects [44,45]. Within this interpretation, one would expect more J/ψ suppression at the LHC since the directly produced J/ψ could be screened at the high-energy density reached in Pb+Pb collisions at the LHC. Quarkonia production has also

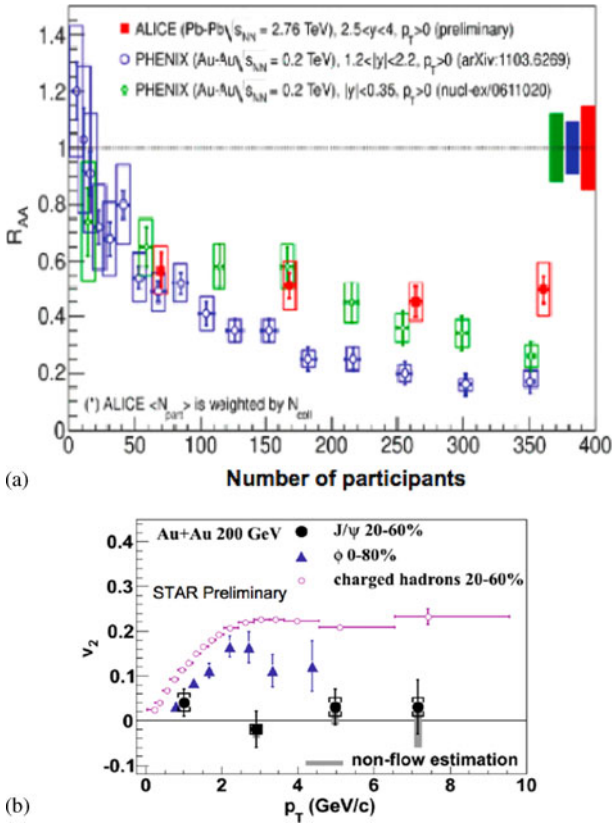

Figure 6. **(a)** Nuclear modification factor R_{AA} for J/ψ as a function of centrality in Au+Au collisions at $\sqrt{s_{NN}} = 200$ GeV from PHENIX [46] and in Pb+Pb collisions at $\sqrt{s_{NN}} = 2.76$ TeV from ALICE [9]. **(b)** J/ψ v_2 (solid circles) as a function of p_{T} in mid-central 20–60% Au + Au collisions at $\sqrt{s_{NN}} = 200$ GeV, where open boxes show systematic uncertainties from non-flow effects, and brackets show those from other sources [49]. Open circles show results of inclusive charged hadrons in 20–60% [50] and solid triangles show the ϕ meson v_2 in 0–80% [51] for comparison.

been studied with a statistical hadronization model which reproduces the available data at RHIC and predicts a large enhancement of $R_{\rm AA}$ of J/ψ at the LHC, due to regeneration [48].

In order to constrain the models and quantify a possible suppression of quarkonia through colour screening, the different sources of suppression (cold nuclear matter effects and other) and enhancement (regeneration) of quarkonia should be systematically disentangled and quantified as a function of rapidity, $p_{\rm T}$ and centrality at each collision energy, using d+Au or p+Au data and models.

Figure 5b shows that the $R_{\rm AA}$ factor at RHIC at midrapidity measured as a function of centrality of the collision is similar to $R_{\rm AA}$ measured at SPS in Pb+Pb collisions at $\sqrt{s_{NN}} = 17$ GeV. In first approximation this is not as expected for suppression of directly produced J/ψ due to colour screening. However, again in this plot suppression effects other than screening, like cold nuclear matter effects have not been corrected out.

Figure 6 shows a comparison of RHIC to LHC $R_{\rm AA}$ factor for J/ψ production as a function of centrality. The $R_{\rm AA}$ factor for J/ψ measured by ALICE in Pb+Pb collisions at $\sqrt{s_{NN}} = 2.76$ TeV at $2.5 < y < 4$, is larger than for J/ψ measured by PHENIX in Au+Au collisions at $\sqrt{s_{NN}} = 200$ GeV at both rapidities shown here, namely $|y| < 0.35$ and $1.2 < |y| < 2.2$. The data in this figure have no $p_{\rm T}$ cut, $p_{\rm T} > 0$. This enhancement of J/ψ $R_{\rm AA}$ at low $p_{\rm T}$ at the LHC with respect to RHIC, suggest possible J/ψ regeneration at LHC.

In the following we discuss the $p_{\rm T}$ dependence of J/ψ suppression pattern. Figure 7a shows the $p_{\rm T}$ spectra of J/ψ in Au+Au collisions at $\sqrt{s_{NN}} = 200$ GeV demonstrating

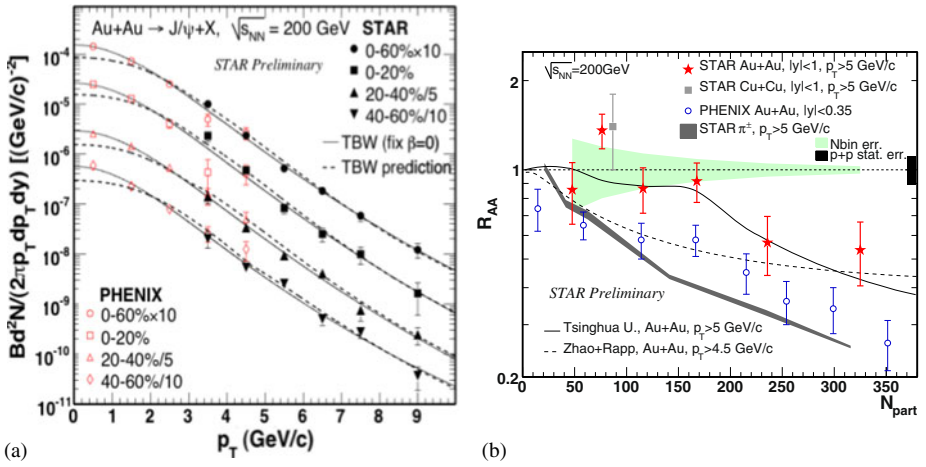

(a) (b)

Figure 7. **(a)** Invariant yields of J/ψ as a function of $p_{\rm T}$ for several different centrality bins shown by solid symbols in Au+Au collisions at $\sqrt{s_{NN}} = 200$ GeV. Open symbols are the published PHENIX results for comparison [55]. Lines are calculations from Tsallis-Blast-Wave model [56]. **(b)** $R_{\rm AA}$ vs. $N_{\rm part}$ for J/ψ at high $p_{\rm T} >$ 5 GeV/c (stars for Au+Au and one grey rectangle for Cu+Cu collisions) and J/ψ at low $p_{\rm T} =$ 0–5 GeV/c in Au+Au collisions (open circles) measured by PHENIX, and high $p_{\rm T}$ pions (dark thick line). The solid and dashed thin lines show two theoretical calculations (see [52] for details).

that PHENIX and STAR agree in the overlap region and combine nicely the low p_T and high p_T acceptance to offer a J/ψ measurement at RHIC with a large coverage in p_t. As shown in figure 7b the R_{AA} factor for J/ψ has been found to be suppressed in central Au+Au collisions at $p_T > 5$ GeV/c by STAR, while it exhibits a larger suppression (a smaller R_{AA}) at smaller p_T (shown by the open circles measured by PHENIX) [52]. The J/ψ measurement in peripheral Au+Au collisions is consistent with the previous STAR measurement in Cu+Cu collisions at the same p_T and at the same number of participant nucleons [53].

The J/ψ measured by STAR at $p_T > 5$ GeV/c and in central Au+Au collisions is less suppressed than the J/ψ measured by CMS in Pb+Pb collisions at $\sqrt{s} = 2.76$ TeV at $p_T > 6.5$ GeV/c and also at midrapidity [54]. Therefore, the collision energy dependence of J/ψ at high p_T from RHIC to LHC seems consistent with a larger system size and/or a larger initial energy density reached at the LHC.

A different amount of J/ψ regeneration at RHIC and LHC energies would influence the J/ψ energy dependence. STAR has measured the elliptic flow of J/ψ (figure 6b) to be consistent with zero in the p_T range 2–8 GeV/c in mid-central Au+Au collisions at 200 GeV [49]. This measurement does not favour J/ψ production dominantly through coalescence from thermalized c and $\bar{c}$ at RHIC, assuming that charm quarks exhibit elliptic flow.

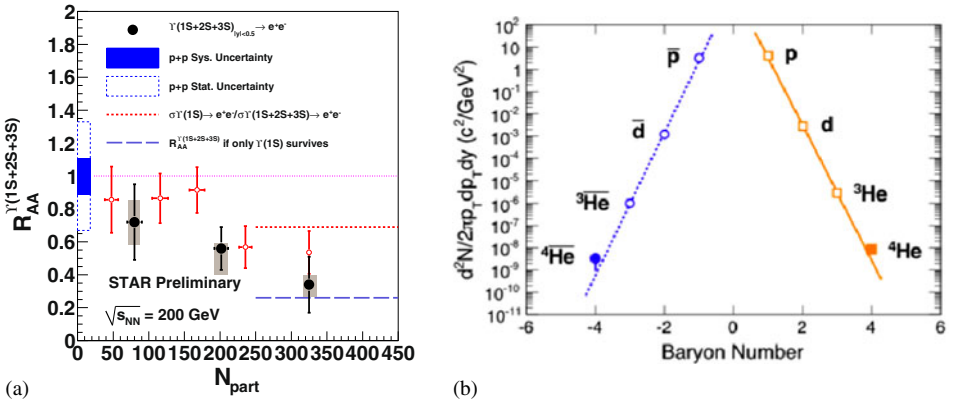

Figure 8. **(a)** R_{AA} of Υ(1S+2S+3S) states as a function of the number of participants in Au+Au collisions at $\sqrt{s_{NN}} = 200$ GeV [57]. The solid black points are the Υ results, the red open points are the high $p_T > 5$ GeV/c J/ψ results. The blue boxes at (0,1) represent the systematic and statistical uncertainty from the $p + p$ cross-section applying to all shown Υ points, while the grey boxes around the Υ points are the systematic uncertainties from other sources (see [57] for details). The red dotted line is the ratio of the total cross-section of Υ(1S) over Υ(1S+2S+3S). The purple dashed line is the ratio of only the direct Υ(1S) cross-section over the total Υ(1S+2S+3S). **(b)** Differential invariant yields as a function of baryon number B, evaluated at $p_T/|B| = 0.875$ GeV/c, in central 200 GeV Au+Au collisions [58]. The lines represent exponential fits. For more details, see [58]. Errors are statistical only. Systematic errors are smaller than the symbol size, and are not plotted.

Furthermore, STAR has measured the suppression of Υ states (1S+2S+3S) (figure 8a) in central Au+Au collisions at 200 GeV for the first time at RHIC [57]. This suppression is consistent with the suppression of the 2S and 3S Υ states and only the 1S Υ state surviving. This hierarchy of suppression is expected within a colour screening senario due to the higher dissociation temperature $T_{\text{dissociation}} > 4T_{\text{critical}}$ of the Υ(1S) state [44,45]. The dissociation temperature of the Υ(2S) state is $1.6T_c$ while for the Υ(3S) state it is $1.17T_c$. An indication of a suppression of the (2S+3S) Υ states over the 1S Υ state suppression has also been observed in Pb+Pb over $p + p$ collisions at the LHC [59].

Further interpretation of the quarkonia suppression pattern requires estimation of cold nuclear matter and other non-colour-screening suppression effects as well as of regeneration effects quantified with d+Au and p+Au collision data as a function of rapidity, p_T, centrality and energy. Also the feeding corrections and cuts should be the same for comparison of data from different experiments.

6. Antimatter

STAR has reported recently in a publication in *Nature* the first observation of antihelium-4 [58]. The antihelium-4 yields measured are important for background estimates of antimatter in space.

7. Beam energy scan

The goal of the beam energy scan (BES) established at RHIC using Au+Au collisions reaching down to $\sqrt{s_{NN}} = 7.7$ GeV is to measure with precision the critical parameters of the phase transition, to discover a possible critical point and map out the QCD phase diagram [60]. One strategy in search of the T_c concerns the search for the turn-off of certain QGP signatures observed at high energy when the energy near T_c is approached from above. Another strategy in the search for the QCD critical point concerns the search for new signatures and new phenomena like enhanced fluctuations, resulting from being in the vicinity of the critical point.

PHENIX has measured recently the evolution of R_{AA} factor with decreasing collision energy, searching at which collision the jet quenching of mesons observed in high-energy Au+Au collisions at high p_T possibly ceases to exist. These data are very important to constrain models of energy loss. Figure 9a shows R_{AA} factor of π^0 mesons in Au+Au collisions in three different energies. A smooth behaviour of R_{AA} is observed: the lower the energy, the smaller the suppression or possibly the higher the p_T required to obtain the same suppression. However, the value of R_{AA} is a convolution of energy loss and other effects like the inverse slope of the spectrum, different PDFs, different contributions from the Cronin effect, and different contributions from soft and hard scattering.

One of the most important findings at RHIC is the universal scaling observed in the elliptic flow coefficient v_2 per constituent quark as a function of p_T per constituent quark among light flavour mesons and baryons in the intermediate p_T region in $A + A$ collisions at RHIC, which is suggested by parton coalescence and recombination models [61]. This

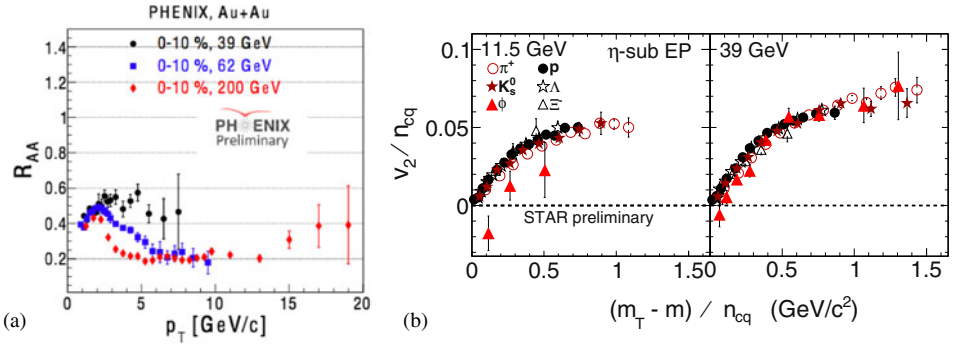

Figure 9. **(a)** R_{AA} as a function of p_{T} for three different energies in Au+Au collisions measured by PHENIX [29]. **(b)** v_2 scaled by the number of constituent quarks (n_{cq}) as a function of $m_{\mathrm{T}} - m$ over n_{cq} for various particles in Au+Au collisions measured by STAR [62].

scaling is a strong indication of partonic degrees of freedom in the early stage of heavy-ion collisions at RHIC. STAR has searched with the beam energy scan to find the energy at which the v_2 scaling is modified or ceases to exist.

The elliptic flow coefficient v_2 of ϕ meson, measured up to $p_{\mathrm{T}} = 2$ GeV/c at $\sqrt{s_{NN}} = 11.5$ GeV, shows a deviation from the v_2 of other hadrons in Au+Au collisions at $\sqrt{s_{NN}} = 11.5$ GeV (figure 9b) [62]. The ϕ meson has been measured from STAR to freeze-out close to the transition temperature predicted by lattice QCD [63] since its interaction with nucleons is smaller compared to other hadrons. The deviation observed in the v_2 of the ϕ in Au+Au collisions at 11.5 GeV indicates a decrease of collectivity resulting from partonic interactions, below a certain energy threshold.

Furthermore, the difference of v_2 between particles and antiparticles measured by STAR is found to be weakly dependent on energy from $\sqrt{s_{NN}} = 39$ GeV on, while it shows a significant deviation at energies lower than $\sqrt{s_{NN}} = 11.5$ GeV (figure 10a), which increases with decreasing energy [62]. These data demonstrate a deviation from the number of constituent quarks scaling of v_2 observed at the highest energies at RHIC below a certain collision energy. The exact collison energy where this change takes place has to be defined through more data at different energies.

Higher moments of fluctuations for conserved quantities like net baryons, are expected to be sensitive to the correlation length of the system, and thus can be used in the search for the critical point [64,65]. Figure 10a shows the excitation function of the product of net-proton (number of protons minus the number of antiprotons) higher moments $S\sigma$ and $\kappa\sigma^2$ in the most central Au + Au collisions, where σ^2, S and κ are the variance, skewness and kurtosis, respectively [66]. Calculations from a hadron resonance gas (HRG) [67] model as well as from lattice QCD [68] are shown for comparison.

A non-monotonic variation with $\sqrt{s_{NN}}$ can indicate the presence of a critical point. It is observed that the data at $\sqrt{s_{NN}} = 62.4$–200 GeV are consistent with both models, while the data show a deviation from the HRG model below $\sqrt{s_{NN}} = 39$ GeV. The statistical uncertainty is expected to be improved in the future with much higher statistics in particular at $\sqrt{s_{NN}} = 19.6$ GeV and 27 GeV.

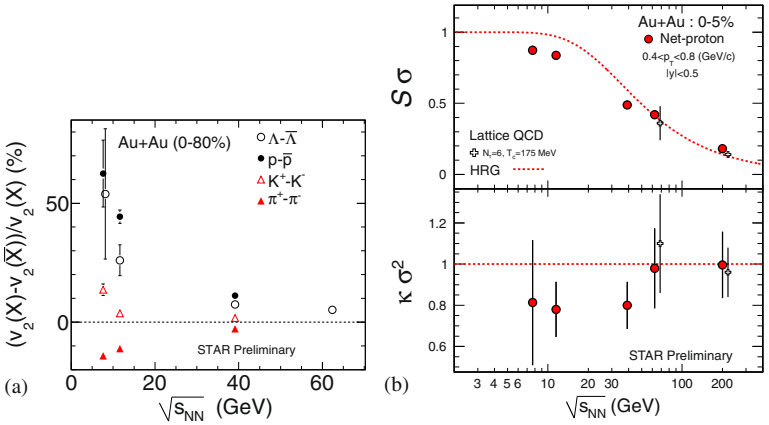

Figure 10. **(a)** The difference of v_2 for particles and antiparticles divided by the particle v_2 as a function of collision energy in Au+Au collisions [62]. **(b)** Product of higher moments $S\sigma$ (top) and $\kappa\sigma^2$ (bottom) for net protons as a function of $\sqrt{s_{NN}}$ in the most central Au+Au collisions [49]. Dashed lines show the calculations from hadron resonance gas model and open crosses show the lattice QCD calculations (see text for more details).

8. Conclusions and outlook

The STAR and PHENIX experiments at the Relativistic Heavy-Ion Collider enter a new era of high precision measurements with major upgrades in detectors and accelerator. RHIC experiments have discovered a strongly interacting quark gluon plasma (sQGP) phase build in central Au+Au collisions at $\sqrt{s_{NN}} = 200$ GeV and aim to measure its characteristics, discover a possible critical point and map out the QCD phase diagram. We reported on measurements by PHENIX of the initial temperature of 300–600 MeV of the sQGP in central Au+Au collisions at $\sqrt{s_{NN}} = 200$ GeV via direct photons. The viscosity-to-entropy ratio has been constrained via PHENIX measurement of flow coefficients and is compatible with the value of $\eta/s = 1/4\pi$ as expected from AdS/CFT. Furthermore, flow coefficients measured by PHENIX suggest a cubic path length dependence of jet quenching, as expected from AdS/CFT.

Open beauty is found to be suppressed in central Au+Au collisions at $p_{\mathrm{T}} > 5$ GeV/c as well as open charm. RHIC experiments performed detailed measurements of J/ψ in $p + p$, d+Au and Au+Au collisions towards understading the origin of its suppression in central Au+Au collisions. A suppression of Υ(1S+2S+3S) states has been recently observed by STAR in central Au+Au collisions compatible with full suppression of only the 2S+3S states, as expected in case of suppression due to colour screening. The understanding of the energy, rapidity and p_{T} dependence of quarkonia requires systematic measurements in d+Au and p+Au collisions.

The first observation ever of antihelium-4 has been made by STAR in Au+Au collisions at 200 GeV setting the background for antimatter observations in space. The beam energy scan program at RHIC is well under way and important results have been reported, such as deviation from the v_2 scaling at low energies. Some STAR and PHENIX short

term main upgrades include silicon detector upgrades, already installed in PHENIX and well underway in STAR and a muon detector for STAR, while long term plans concern optimization for $e + A$ data taking towards e-RHIC.

References

[1] Wuppertal-Budapest Collaboration: Szabolcs Borsanyi *et al*, *J. High Energy Phys.* **1009**, 073 (2010), e-Print: arXiv:1005.3508 [hep-lat]
[2] U Heinz and M Jacob, arXiv:0002041, nucl-th
[3] P Braun-Munzinger, J Stachel, J P Wessels and N Xu, *Phys. Lett.* **B344**, 43 (1995), arXiv:nucl-th/9410026
[4] F Becattini, J Cleymans, A Keranen, E Suhonen and K Redlich, *Phys. Rev.* **C64**, 024901 (2001), arXiv:hep-ph/0002267
[5] R Hagedorn, CERN-TH-4100/85 (1985)
[6] PHENIX Collaboration: S Bathe *et al,* Quark Matter (2011)
[7] PHENIX Collaboration: A Adare *et al, Phys. Rev. Lett.* **104**, 132301 (2010)
[8] *Nucl. Phys.* **A757**, 1; 102; 184; 28 (2005)
[9] T Nayak, *These proceedings*
[10] Marek Gazdzicki, Mark Gorenstein and Peter Seyboth, *Acta Phys. Polon.* **B42**, 307 (2011), arXiv:1006.1765 [hep-ph]
[11] A Andronic, P Braun-Munzinger and J Stachel, *Nucl. Phys.* **A834**, 237C (2010), arXiv:0911.4931 [nucl-th]
[12] Sonia Kabana and Peter Minkowski, *New J. Phys.* **3**, 4 (2001), e-Print: hep-ph/0010247
[13] Sonia Kabana, *Eur. Phys. J.* **C21**, 545 (2001), e-Print: hep-ph/0104001
[14] PHENIX Collaboration: T Sakaguchi, *Nucl. Phys.* **A855**, 141 (2011), arXiv:1012.1893
[15] PHENIX Collaboration: A Adare *et al,* arXiv:1105.4126 [nucl-ex]
[16] J Y Ollitrault, *These proceedings*
[17] PHENIX Collaboration: S S Adler *et al*, *Phys. Rev. Lett.* **91**, 182301 (2003)
[18] PHENIX Collaboration: A Adare *et al,* Submitted for publication in *Phys. Rev. Lett.*, arXiv:1105.3928 [nucl-ex]
[19] B H Alver, C Gombeaud, M Luzum and J Y Ollitrault, *Phys. Rev.* **C82**, 034913 (2010), arXiv:1007.5469 [nucl-th]
[20] B Alver, M Baker, C Loizides and P Steinberg, arXiv:0805.4411 [nucl-ex]
[21] T Lappi and R Venugopalan, *Phys. Rev.* **C74**, 054905 (2006)
[22] H J Drescher and Y Nara, *Phys. Rev.* **C76**, 041903 (2007)
[23] P Sorensen, *J. Phys.* **G37**, 094011 (2010)
[24] B Alver and G Roland, *Phys. Rev.* **C81**, 054905 (2010), Erratum, *ibid.* **C82**, 039903 (2010)
[25] G Policastro, D T Son and A O Starinets, *Phys. Rev. Lett.* **87**, 081601 (2001), arXiv:hepth/0104066
[26] P Kovtun, D T Son, A O Starinets, *Phys. Rev. Lett.* **94**, 111601 (2005), [hep-th/0405231]
[27] D Kharzeev *et al*, *Phys. Lett.* **B519**, 1999 (2001), arXiv:hep-ph/0106202
[28] M Djordjevic *et al*, *Phys. Rev. Lett.* 94 (2004)
[29] PHENIX Collaboration: M Purschke *et al*, Quark Matter (2011)
[30] PHENIX Collaboration: A Adare *et al*, *Phys. Rev. Lett.* **105**, 142301 (2010)
[31] A Drees, H Feng and J Jia, *Phys. Rev.* **C71**, 034909 (2005), arXiv:nucl-th/0310044
[32] J Jia and R Wei, *Phys. Rev.* **C82**, 024902 (2010)
[33] PHENIX Collaboration: A Adare *et al*, *Phys. Rev.* **C84**, 044905 (2011), e-Print: arXiv:1005.1627 [nucl-ex]
[34] S Wicks, W Horowitz, M Djordjevic and M Gyulassy, *Nucl. Phys.* **A784**, 426 (2007)

[35] C Marquet and T Renk, *Phys. Lett.* **B685**, 270 (2010)
[36] S S Gubser, D R Gulotta, S S Pufu and F D Rocha, *J. High Energy Phys.* **0810**, 052 (2008)
[37] P M Chesler, K Jensen, A Karch and L G Yaffe, *Phys. Rev.* **D79**, 125015 (2009)
[38] F Dominguez, C Marquet, A H Mueller, B Wu and B W Xiao, *Nucl. Phys.* **A811**, 197 (2008)
[39] PHENIX Collaboration: S S Adler *et al*, *Phys. Rev. Lett.* **96**, 032301 (2006)
[40] STAR Collaboration: B I Abelev *et al*, *Phys. Rev. Lett.* **98**, 192301 (2007), Erratum, *ibid.* **106** 159902 (2011), e-Print: nucl-ex/0607012
[41] PHENIX Collaboration: C da Silva *et al*, *Proceedings of the International Conference on Quark Matter* (Annecy, 2011) Quark Matter (2011)
[42] PHENIX Collaboration: A Adare *et al*, *Phys. Rev. Lett.* **103**, 082002 (2009), e-Print: arXiv:0903.4851 [hep-ex]
[43] STAR Collaboration: M M Aggarwal *et al*, *Phys. Rev. Lett.* **105**, 202301 (2010), arXiv:1007.1200
[44] F Karsch, D Kharzeev and H Satz, *Phys. Lett.* **B637**, 75 (2006)
[45] H Satz, *J. Phys.* **G32**, R25 (2006)
[46] PHENIX Collaboration: C L da Silva *et al,* Quark Matter (2011)
[47] PHENIX Collaboration: A Adare *et al*, *Phys. Rev. Lett.* **107**, 142301 (2011), e-Print: arXiv:1010.1246 [nucl-ex]
[48] A Andronic, P Braun-Munzinger, K Redlich and J Stachel, *J. Phys.* **G G37** 094014 (2010), e-Print: arXiv:1002.4441 [nucl-th]
[49] STAR Collaboration: H Masui *et al*, Quark Matter (2011)
[50] STAR Collaboration: J Adams *et al, Phys. Rev. Lett.* **93**, 252301 (2004)
[51] STAR Collaboration: B I Abelev *et al*, *Phys. Rev. Lett.* **99**, 112301 (2007)
[52] STAR Collaboration: Z Tang *et al,* Quark Matter (2011)
[53] STAR Collaboration: B Abelev *et al, Phys. Rev.* **C80**, 041902 (2009)
[54] CMS Collaboration: Bolek Wyslouch *et al, J. Phys.* **G38**, 124107 (2011)
[55] PHENIX Collaboration: A Adare *et al*, *Phys. Rev. Lett.* **98**, 232301 (2007)
[56] Z Tang *et al,* arXiv:1101.1912 [nucl-ex]
[57] STAR Collaboration: R Reed *et al*, Quark Matter (2011)
[58] STAR Collaboration: H Agakishiev *et al*, *Nature* **473**, 353 (2011)
[59] CMS Collaboration: *Phys. Rev. Lett.* **107**, 052302 (2011)
[60] STAR Collaboration: L Kumar *et al*, *J. Phys.* **G38**, 124145 (2011), arXiv:1106.6071; iB. STAR Collaboration: Mohanty *et al*, *J. Phys.* **G38**, 124023 (2011), e-Print: arXiv:1106.5902 [nucl-ex]
[61] STAR Collaboration: J Adams *et al*, *Phys. Rev. Lett.* **93**, 252301 (2004)
STAR Collaboration: B I Abelev *et al, Phys. Rev. Lett.* **99**, 112301 (2007)
D Molnar and S A Voloshin, *Phys. Rev. Lett.* **91**, 092301 (2003)
V Greco, C M Ko and P Levai, *Phys. Rev.* **C68**, 034904 (2003)
[62] STAR Collaboration: B Mohanty *et al*, Quark Matter (2011)
[63] STAR Collaboration: J Adams *et al, Nucl. Phys.* **A757**, 28 (2005)
[64] M A Stephanov, *Phys. Rev. Lett.* **102**, 032301 (2009)
[65] STAR Collaboration: M M Aggarwal *et al*, *Phys. Rev. Lett.* **105**, 022302 (2010)
[66] STAR Collaboration: T Tarnowsky, Quark Matter (2011)
[67] F Karsch and K Redlich, *Phys. Lett.* **B695**, 136 (2011)
[68] S Gupta, X Luo, B Mohanty, H G Ritter and N Xu, *Science* **332**, 1525 (2011)